



Organo-nano bentonite and organo-nanokaoline for effective removal of Pb(II) ions from battery effluent: characterization, isotherm, kinetic studies

B. Uma Maheswari, V.M. Sivakumar*, M. Thirumarimurugan

Department of Chemical Engineering, Coimbatore Institute of Technology, Coimbatore 641014, India,
email: umasuresh16@gmail.com (B. Uma Maheswari), vmsivakumar@gmail.com, vmsivakumar@cit.edu.in (V.M. Sivakumar),
thirumarimurugan@gmail.com (M. Thirumarimurugan)

Received 18 July 2018 ; Accepted 23 December 2018

ABSTRACT

Lead is considered as one of the deadliest heavy metals which causes severe impact on the environment. In the present work, the experimental study was carried out by using eco-friendly nano-adsorbent material ONK (organo-nanokaoline) and ONB (organo-nanobentonite) for the effective removal of Pb(II) ions from battery synthetic effluent. The organically modified adsorbents were characterized by Fourier transform infrared spectroscopy (FTIR), X-ray diffraction (XRD), scanning electron microscope (SEM), energy dispersive X-ray (EDX), thermogravimetric analysis (TGA). Operating parameters such as pH, adsorbent dosage and contact time were experimentally optimized for the maximum removal of ions. The optimum conditions were found to be at pH of 4, a dosage of 4 g/L, 30 min equilibrium time with 400 mg/L initial concentration for ONK. The adsorption data was fitted with isotherm models such as Langmuir and Freundlich. The monolayer adsorption capacity of ONK and ONB for Pb(II) ions was reported to be about 47 mg/g (ONK), 32 mg/g (ONB), respectively. Adsorption kinetics and mechanism were analyzed using pseudo-first order, pseudo-second order, intra particle diffusion model, and Boyd model. The pseudo second order kinetic model provided the best fit for absorption of ions.

Keywords: Lead; ONB; ONK; Isotherm; Kinetics

1. Introduction

Due to the rapid growth of industries, heavy metal pollution has become one of the most important environmental problems today. Water gets polluted mainly because of toxic contaminants released by the industries, anthropogenic activities, and environmental changes. The presence of heavy metal ions beyond the permissible limit is a serious environmental issue because of its non-biodegradable nature [1]. The major sources of environmental pollution are due to excess amount of metal ions released from industries such as textile, leather, electroplating, galvanizing, dyes, pigments mining, metal finishing, metal processing industries [2]. Lead, nickel, chromium, zinc, cadmium and copper are stable carcinogenic heavy metals [3–8]. The impact of heavy metal releases in the environment is severe, that has become a threat to human and aquatic life. Toxic elements may bio-accumulate

and may also affect the food chain in the living organisms [9]. Among these, lead ions are deemed to be highly toxic, even at low concentration [10]. Generally, industrial waste water contains 5–15 mg/L of Pb(II) ions. But as per US Environmental Protection Agency (USEPA) and Bureau of Indian Standards (BIS), the limits of Pb(II) ions are within the level of 0.05 mg/L in drinking water [11]. Even a trace of exposure to such heavy metals can cause serious health illness such as lung irritation, kidney disorder, liver damage, mental retardation, bone cancer, anemia, and intellectual disability in humans [12]. Unit operation such as adsorption, flocculation, solvent extraction, electro dialysis, co-precipitation, and chelation therapy are some of the methodologies that have been followed for the treatment of Pb(II) removal from wastewater. Among these methods, adsorption is recommended as an efficient, versatile and economically feasible method for the removal of Pb(II) ions from waste water [13]. A number of low cost adsorbents such as *S.potatorum* [14], granulated

*Corresponding author.

Presented at the InDA Conference 2018 (InDA CON-2018), 20–21 April 2018, Tiruchirappalli, India

activated carbon [15], bael leaf powder [16], cashew nut shell [17,18], chitosin-polyacrylonitrile (PAN), polyvinyl alcohol (PVA), nanocomposite [19–21], corn cobs [22], wheat pulp [23] have been employed for the removal of Pb(II) ions from aqueous solution. But considering the complexity of waste disposal, in addition to scientific predilection, reusability and economic considerations play a vital role in the selection of adsorbent for pollution decrement. Thus, many researchers are focusing on the cost-effective, eco-friendly adsorbents.

In recent years, clay is widely used as an adsorbent in the removal of heavy metals due to its low-cost, abundant efficiency and economic feasibility. However, many studies have been reported on the removal of heavy metals by bentonite [24–28], kaoline [29–34] and the application of the pure form of the clay is not efficient and it is time-consuming in terms of removal. Presently, researchers are concentrating on organoclays in which the sorption characteristics of clay materials are replaced by natural inorganic inter-layer cation with selected organic cations [35]. Generally, clay minerals are hydrophilic. In order to render the surface to organophilic, hydrated cationic surface are replaced by cationic surfactants such as alkyl ammonium or alkyl phosphonium to reduce the surface energy. The cations receding between the layers, make the organic molecule to radiate away automatically that leads to an increase in the inter-layer spacing between the platelets. [36,37]. Based on the cation exchange reactions, involving the exchange of quaternary alkyl ammonium cations with interlayer cations of the clay mineral in aqueous solution, organo clays are prepared. The properties of organoclay strongly depend on the nano and micro-structural arrangement of the hybrid materials. These surfactant modified clays possess very high specific area and high adsorption capacity, making the clay mechanically and chemically stable [38]. Modification of organonano can be done by treating the clay with suitable surfactant cations such as hexadecyltrimethylammonium (HDTMA), tetra-methyl ammonium (TMA), tetra-ethyl ammonium (TEA), tribenzylmethyl-ammonium (TBMA) so that exchanging of inorganic cations present on the clay surface and within the inter layer space can be increased. Due to these modifications, variation may take place on properties such as surface charge, hydrophobicity and cation exchange capacity of the clays [39]. The application of nano-sized clay was examined due to particular surface characteristics of a nanostructured material along with its larger surface area compared to its original size [40].

The novelty of the present study is the utilization of nanoadsorbents ONK and ONB, to find for the adsorption behavior of Pb(II) ions using battery effluent. The effect of pH, adsorbent dosage, contact time was investigated. In order to comprehend the adsorption mechanism of ONK, ONB, kinetic studies were tested for pseudo-first order, pseudo-second order, intra-particle diffusion, and Boyd kinetic models. The adsorption equilibrium data were analyzed using Langmuir, Freundlich models.

2. Materials and method

2.1. Chemicals

Kaoline and bentonite clay were purchased from Sigma Chemicals, India. Cetyltrimethylammoniumbromide (CTAB) $C_{19}H_{42}BrN$ was used as a surfactant. All the chemicals used in this study were of analytical grade (99%) pure. The cation exchange capacity of kaolin clay was 89 mmol/kg, while that of modified clay was 240 mmol/kg. Similarly, cation exchange capacity of bentonite was 83 mmol/kg, while that of modified clay was 223 mmol/kg. The ion exchange capacities of clays were analyzed by the method of using ammonium chloride and ammonia [34].

2.2. Preparation of organo-nanokaolineclay (ONK) and organo-nanobentonite clay (ONB)

2.2. Preparation of organo-nanokaolineclay (ONK) and organo-nanobentonite clay (ONB)

About 4% w/w clay (Na-Kaoline and Na-Bentonite) was dispersed in 500 ml distilled water with the agitation of about 30 min. Using magnetic stirrer, the suspension was stirred for 24 h at room temperature. CTAB was gradually added to the suspension (ONK, ONB), again the mixture was further stirred and it was allowed to settle for 12 h. The suspended product was filtered under vacuum, using Whatman paper no 1. The resultant product was dispersed in 50 ml fresh distilled water and stirred for 2 h. The resultant modified clay was washed thoroughly to remove chloride and it was confirmed by checking against silver nitrate solution [36]. The final modified clay was dried at 70°C, sieved using BSS 230, and finally grounded using mortar in order to obtain a fine powder.

2.3. Material characterization studies

The X-ray diffraction (XRD) studies of clay and modified clay were performed with XPERT Philips X-ray diffractometer. All parameters were obtained using Cu/ $K\alpha$ radiation operated at 45 KV and 30 mA. The surface morphology of kaoline, bentonite, organo-nanokaoline, and organo-nanobentonite was analyzed using scanning electron microscope (SEM) (Philips-EEI ESEM-TEP, Holland). SEM images were further supported by energy dispersive X-ray (EDX) micro analysis to detect the evidence for purity and distribution of specific elements in solid samples. In order to study the characterization of the functional groups, fourier transform infrared spectroscopy (FTIR) spectra of adsorbent samples were recorded on Bruker Optics spectrometer. The spectra were collected over the range from 400 to 4000 cm^{-1} . The thermal stability of the prepared adsorbents (ONK, ONB) was studied using thermogravimetric analyzer (TGA) model NETZSCH STA 409/CD using purified nitrogen as a carrier gas in the temperature range of 30°–1000°C.

2.4. Adsorption (batch) experiment

Batch adsorption studies were performed in 250 ml flask at room temperature for varying time intervals with 50 ml of the 400 mg/L metal solution, 4 g/L of (ONK, ONB) adsorbent material maintaining a pH of 4 (ONK), 5 (ONB) in the solution. The flask containing solution was placed in an incubator shaker (Orbital Incubator Shaker, Royal Testing Equipment, Chennai, India) at 200 rpm for about 1–2 h. After the adsorption process, the spent ONK and ONB was separated from the solution by centrifuging process (2500

rpm, 10 min) and the final concentration of Pb(II) ions left in the solution was determined by using flame atomic absorption (FAA) spectrophotometer. The removal efficiency of Pb(II) ions was calculated by the following equation

$$\text{Removal efficiency} = \frac{C_i - C_e}{C_i} * 100 \quad (1)$$

where C_i and C_e are the initial and final Pb(II) ion concentration in the solution (mg/L), respectively.

2.4.1. Adsorption isotherm

The adsorption equilibrium data were fitted by two different isotherm models such as Langmuir [41] and Freundlich models [42]. Langmuir isotherm assumes the uptake of metal ions that occurs on a homogenous surface by monolayer adsorption without any interaction between the adsorbed ions. It is represented in the following equation

$$\frac{C_e}{q_e} = \frac{1}{q_m b} + \frac{C_e}{q_m} \quad (2)$$

and separation parameter (R_L) is given by Eq. (3)

$$R_L = \frac{1}{1 + bC_i} \quad (3)$$

Based on the adsorption on heterogeneous surface, Freundlich isotherm given in Eq. (4) is being used.

$$\log q_e = \log K_f + \frac{1}{n} \log C_e \quad (4)$$

where q_e denote the adsorption capacity at equilibrium (mg/g), q_m is the maximum monolayer adsorption capacity (mg/g), b (L/mg) is the Langmuir constants. K_f ($\text{mg}^{1-1/n} \text{L}^{1/n} \text{g}^{-1}$) is Freundlich constant corresponds to bonding energy and n is the measure of the deviation from linearity of adsorption.

2.4.2. Adsorption kinetics and mechanism

Adsorption kinetics studies were performed by mixing 4 g/L of ONB, ONK with 50 ml Pb(II) ion solution with the concentration of 400 mg/L at a pH of 4 for ONK and 5 for ONB in a stoppered conical flask. The conical flask was placed in an incubator shaker. 10 ml of the sample was withdrawn from a same conical flask at time intervals ranging from 10 to 90 min, then centrifuged and finally the residual Pb(II) ion concentration was determined. The amount of Pb(II) ions (q_t) adsorbed onto the ONK and ONB at time t , q_t (mg/g) was estimated by the following equation

$$q_t = \frac{(C_i - C_t)V}{m} \quad (5)$$

where C_t is the concentration of Pb(II) ions at time t in mg/L, V is the volume of the Pb(II) solution (L), m is the mass of adsorbent (ONB, ONK) used (g). Adsorption kinetic data were applied to pseudo-first order and pseudo-second order kinetic model in order to determine the adsorption

process. Pseudo- first order model [43] can be represented by the following equation

$$\log(q_e - q_t) = \log q_e - \frac{k_1}{2.303t} \quad (6)$$

where k_1 is the first order rate constant (min^{-1}), ' q_e ' and ' q_t ' are the amount of adsorbate species adsorbed at equilibrium and at any time (mg g^{-1}). k_1 can be obtained from the slope of a linear plot of $\log(q_e - q_t)$ vs t . Pseudo-second order model [44] is denoted by Eq. (7)

$$\frac{t}{q_t} = \frac{1}{k_2 q_e^2} + \frac{1}{q_e} (t) \quad (7)$$

where k_2 is the rate constants of pseudo-second order kinetics equation ($\text{g mg}^{-1} \text{min}^{-1}$). $k_2 q_e^2$ is the initial sorption rate. By plotting (t/q_t) vs. t , q_e (slope) and k_2 (intercept) can be determined. The adsorption mechanism was explained by applying the values of kinetic data in intraparticle diffusion [45] and Boyd kinetic models [46]. The intraparticle diffusion model is given by Eq. (8)

$$q_t = k_p t^{1/2} + C \quad (8)$$

where k_p is the intraparticle diffusion rate constant ($\text{mg/g min}^{0.5}$), t is the time (minutes), C is the constant related to the thickness of the boundary layer. Boyd kinetic models were used to determine the adsorption kinetic data to identify the actual slowest step in the adsorption of Pb(II) ions onto ONK and ONB. The Boyd kinetic Eq. (9) is as follows

$$-0.4997 - \ln(1 - F) = Bt \quad (9)$$

where

$$F = \frac{q_t}{q_e} \quad (10)$$

The effective diffusion coefficient D_i (m^2/s) values were calculated by using Eq. (12)

$$Bt = -0.4977 - \ln(1 - F) \quad (11)$$

$$B = \frac{\pi^2 D_i}{r^2} \quad (12)$$

where D_i is the effective diffusion coefficient of Pb(II) ion onto adsorbent (ONK, ONB) surface, F is the fraction of Pb(II) ion adsorbed onto the adsorbent (ONK, ONB) at any time t . B_i is a mathematical function of F , r is the radius of the adsorbent particle.

3. Results and discussion

3.1. Characterization of adsorbents

The structural modification that occurred in ONB and ONK owing to surface modification treatment was studied using X-ray diffraction analysis. Additionally, the untreated kaoline and bentonite were also analyzed along with organically modified bentonite and kaoline are shown in Figs. 1 and 2, respectively. From Figs. 1 and 2 it is observed from

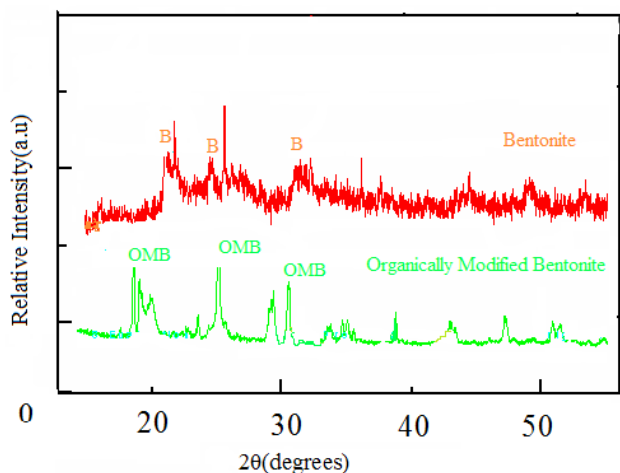


Fig. 1. XRD images of clay (bentonite) and organically modified clay (ONB).

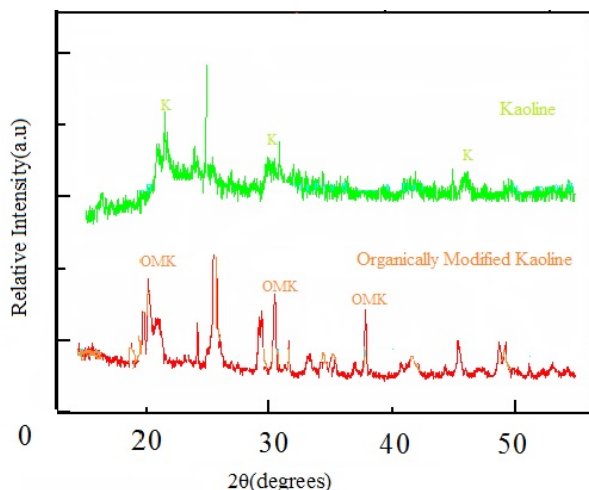


Fig. 2. XRD images of clay (kaoline) and organically modified clay (ONK).

the figures decrease in intensity of the bentonite and kaoline peak $2\theta = 21.27^\circ$, 21.08° correspondingly formation of new peaks at $2\theta = 29.16^\circ$, 29.19° corresponding to ONB, and ONK, respectively. Less intense peaks seen in raw samples indicate the amorphous nature of the adsorbent [47]. The average size of OKN and OBN was assessed using the Debye-Scherrer equation

$$d = \frac{k\lambda}{\beta \cos\theta} \quad (13)$$

In this equation d is the thickness of the crystal, k is the Debye-Scherrer constant (0.9), λ is the X-ray wavelength, β is the peak width with maximum intensity in half height, θ is the diffraction angle. The results obtained from the analysis of XRD pattern by using the Debye-Scherrer equation indicated that the average crystal size for ONK and ONB 23.83 nm, 27.45 nm respectively. Further, the basal spacing of ONB was 0.325 nm ($2\theta = 26.65^\circ$) but the basal spacing of ONK was 0.344 nm, ($2\theta = 25.87^\circ$), indicating that the CTAB surfactant

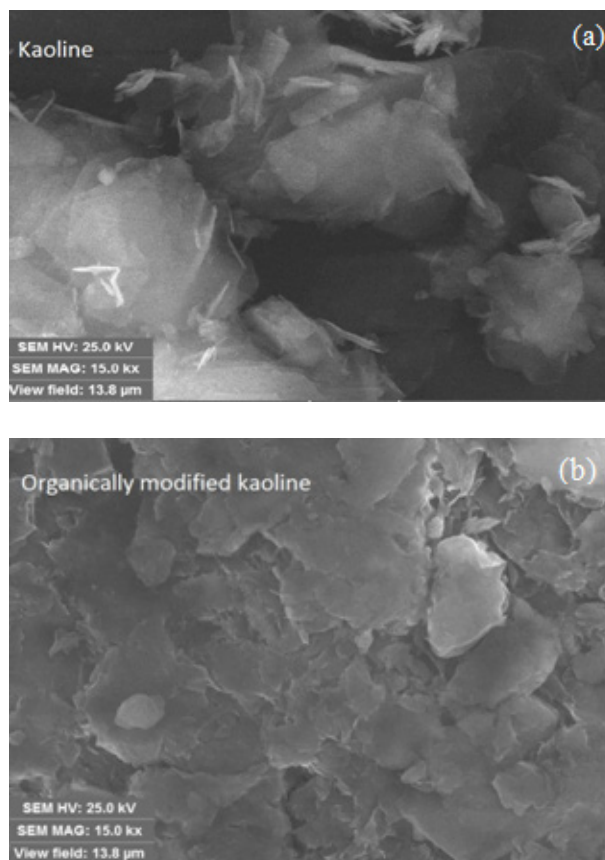


Fig. 3. (a) SEM images of kaoline. (b) SEM images of organically modified clay.

was successfully incorporated in the interlayer of ONK than ONB. The results clearly depict that the amount of added surfactant CTAB has a direct effect on the interlayer expansion of ONK [48]. This confirms that there will be an automatic decrement in the hydration water content. Hence, the surface property of the adsorbent changes from hydrophilic to hydrophobic [39]. Therefore, due to the increase in interlayer space, more spaces will be available for the adsorption of Pb(II) ion, leading to an increase in its removal efficiency.

The surface morphology of ONK and ONB were investigated using SEM, the resulting images are shown in Figs 3a, b, 5a, b. From Fig. 3, bit is seen that the introduction of CTAB in kaoline (ONK) lead to coarse particles and porous surface favors inter layer exchange and inter layer adsorption. This in turn promotes the Pb(II) ion penetration into the galleries of the modified organo-nanokaoline, resulting in an increase in the adsorption capacity of the adsorbent.

Bentonite and its organo-nano form are shown in Figs. 5a,b. The shape of bentonite seems to be formed by dense particles. Bentonite possesses irregular shape where some white particles appeared on the surface of the mineral particle. These are non-clay minerals containing Fe, K, Ti, Mg, Na. After modification using CTAB, the flaky structure of bentonite clay was converted to the fractional and needle-like structure. Contrastively, the ONB possess relatively different surface morphology as seen in Fig. 5b. The bentonite particles are relatively smoother, with small fragmented

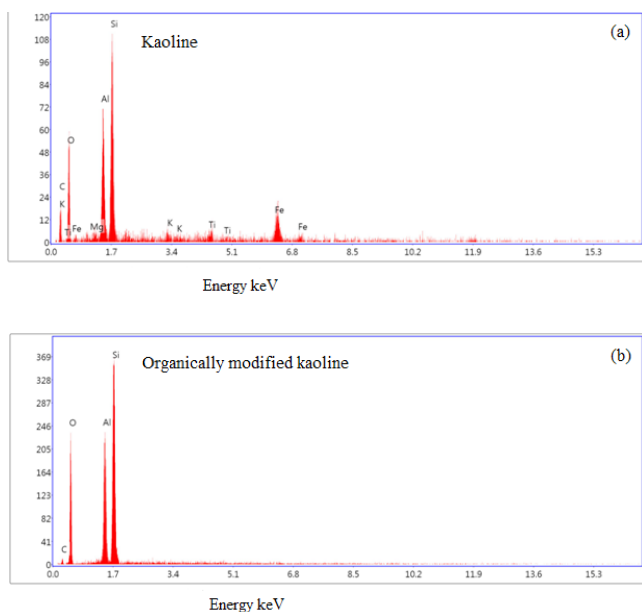


Fig. 4. (a) EDX reports of kaoline (b) EDX reports organically modified clay.

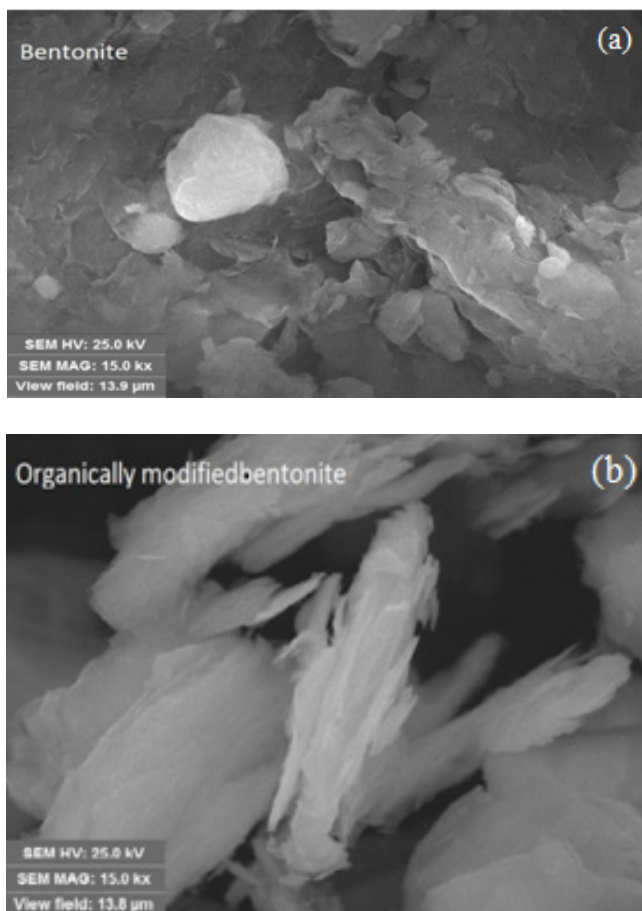


Fig. 5. (a) SEM images of bentonite (b) SEM images of organically modified clay.

Table 1
Elemental composition of ONK, ONB

Elements	Weight percentage of elements	
	ONK (%)	ONB (%)
Si	51.78	47.95
Al	12.21	14.67
O	19.62	27.74
C	15.78	9.64
K	0.61	–

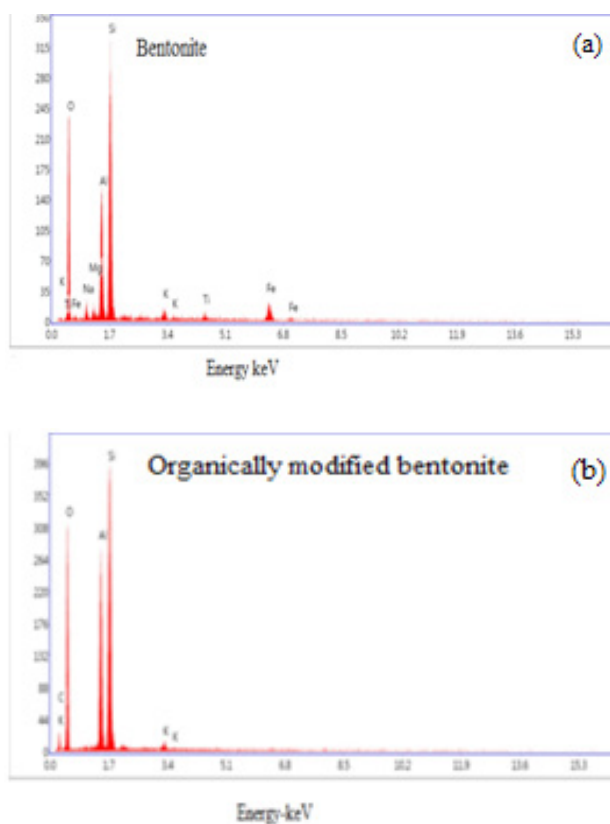


Fig. 6. (a) EDX reports of bentonite (b) EDX reports of organically modified clay.

and block particles adhering to the surface. This may be the reason that ONB has a smaller specific area than ONK, which results in the lower adsorption capacity of ONB. Figs. 4a,b and 6a,b show the EDX analysis of kaoline, ONK, bentonite, ONB. The weight percentage (weight %) of Si, Al, O, C, K within the compounds are depicted in Table 1. From the results, it is evident that ONK and ONB composed of Si compounds are suitable for the adsorption of various organic pollutants [39]. As discussed in SEM analysis, the non-clay minerals containing Fe, K, Ti, Mg, Na are present in the raw sample of kaoline and bentonite.

The band assignments of clay and organically modified clay (ONB, ONK) were analyzed using FTIR spectra. The capacity of the adsorbent mainly depends upon the porosity

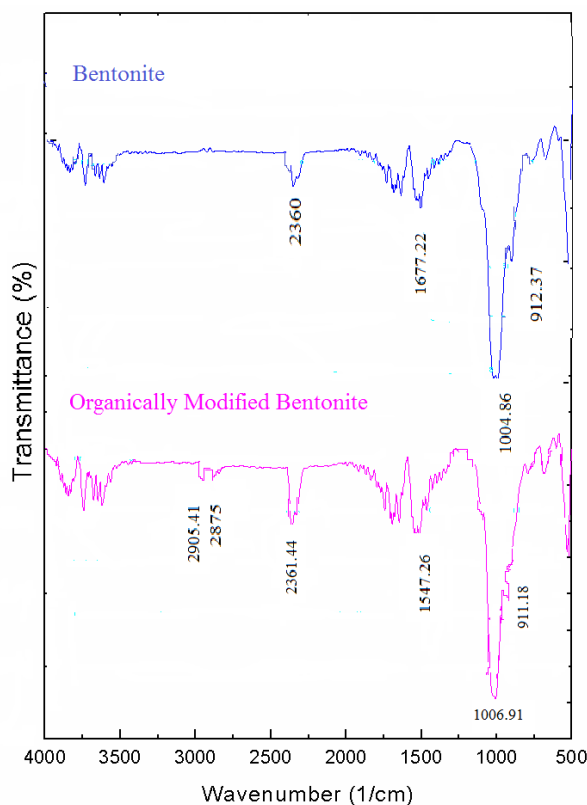


Fig. 7. FTIR images of bentonite and ONB.

and chemical reactivity of the functional groups present on its surface [49]. The results of the FTIR spectra are presented in Figs. 7 and 8. The intense peak 3672.12 cm^{-1} of organically modified kaoline in Fig. 8 is due to O-H stretching of water. Similarly, the presence of Si-O stretching vibrations are also confirmed by 1037.64 cm^{-1} , in ONK, 1006.91 cm^{-1} in ONB. The corresponding CH_2 bending vibrations of ONK and ONB occurred at 1515.48 cm^{-1} , 1547.26 cm^{-1} , respectively. Formation of new peaks in ONB at 2905.41 cm^{-1} , 2875 cm^{-1} clearly indicates the presence of surfactant CTAB in the organically modified adsorbent. The results observed from FTIR studies indicated that both ONK and ONB possess a variety of functional groups such as hydroxyl, carbonyl, silicate, aluminum which may involve in the adsorption of Pb(II) ions.

Thermogravimetric analysis (TGA) was performed upon ONK and ONB samples. The weight loss versus temperature is represented in Figs. 9 and 10. It is noted that TGA of ONB occurred in three mass loss steps at a temperature of 80°C , $280^\circ\text{--}540^\circ\text{C}$ and remained stable still 700°C . These mass loss steps occurrence may be due to desorption of water from the clay, dehydration of cation in the interlayer, and dehydroxylation of ONB. From Fig. 10, it is observed that the four stages of degradation take place in ONK. The first stage of weight loss at 70°C attributed to water desorption. The second stage of hydration of water in the interlayer cation was observed at 210°C – 420°C . The third step till 630°C due to degradation of the CTAB (surfactant). Further, the last stage of dehydroxylation of the clay hydroxyl groups observed up to 840°C .

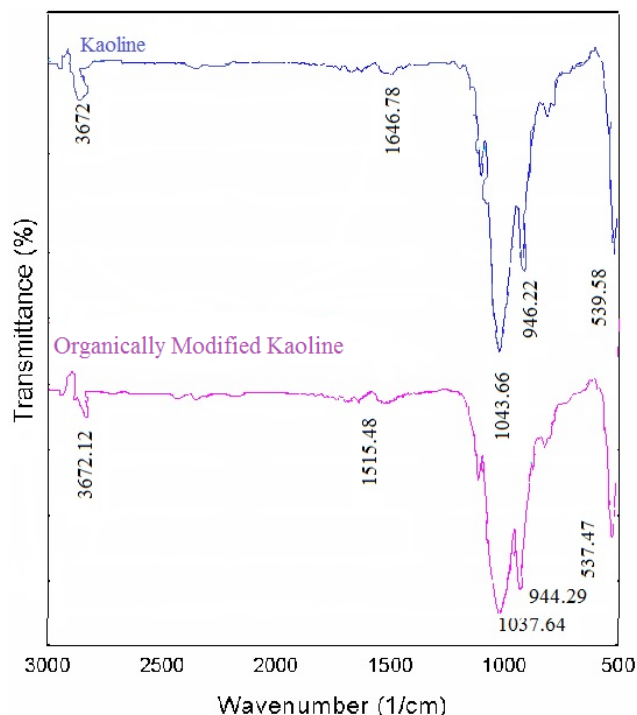


Fig. 8. FTIR images of kaoline and ONK.

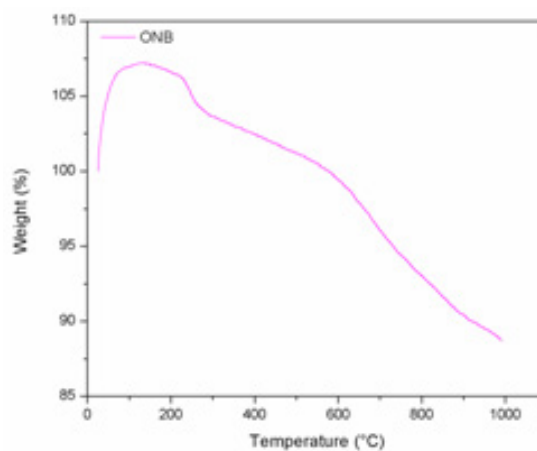


Fig. 9. Thermogravimetric analysis of ONB.

3.2. Effect of pH

pH of a solution is generally influenced by the surface charge and dissociation of the functional group of the adsorbent. Adsorption experiments were performed in the pH range from 2 to 7 for Pb(II) ion concentration 400 mg/L contact time 30 min for ONK and 45 min for ONB. Fig. 11 shows the influence of pH on the adsorption of Pb(II) ions onto the adsorbent material (ONK, ONB). The maximum removal of Pb(II) is attained at a pH of 4.2 for ONK and pH = 5 for ONB after which there is a decrement in the removal of ions. Beyond the pH value of 4 (ONK) and pH value of 5 (ONB), it is observed that metal hydroxide complexes are formed which in turn reduces

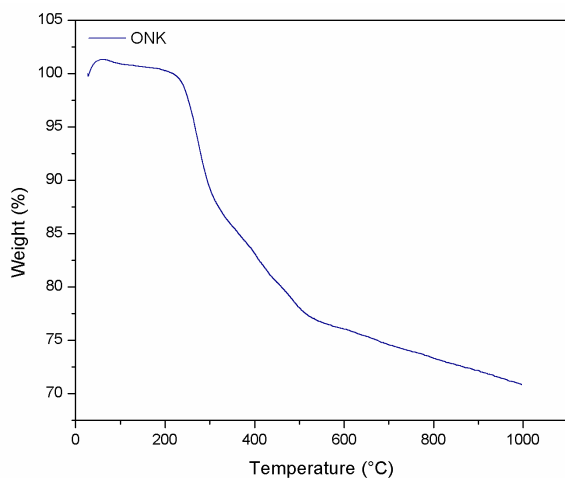


Fig. 10. Thermogravimetric analysis of ONK.

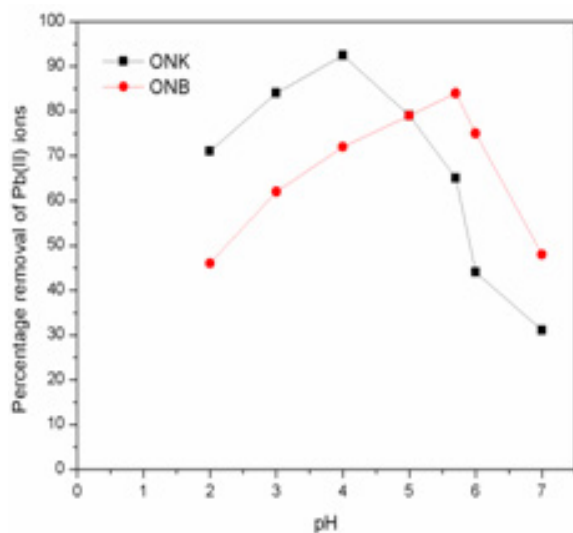


Fig. 11. Effect of pH on the adsorption of Pb(II) ions onto the ONK and ONB.

the adsorption capacity of the adsorbent [3]. Hence, pH = 4 (ONK) and pH = 5 (ONB) are considered to be optimum for experimental studies to avoid the formation of metal hydroxides.

3.3. Effect of adsorbent dosage

The effect of adsorbent (ONK, ONB) was studied by varying the adsorbent dosage from 0.5 to 6 g/L at an initial concentration of 400 mg/L. From Fig. 12 the plot reveals that adsorption of Pb(II) increases as the adsorbent dosage (ONK, ONB) increases from 0.5 to 4 g/L. There is no significant change in the percentage removal of Pb(II) ions. 92.4% (ONK) and 84% (ONB) is observed above 4 g/L of adsorbent dosage. This is probably due to the formation of aggregates of the adsorbents at higher dosages and limited availability of the number of adsorbing species to the relatively large number of surface sites on the increasing the

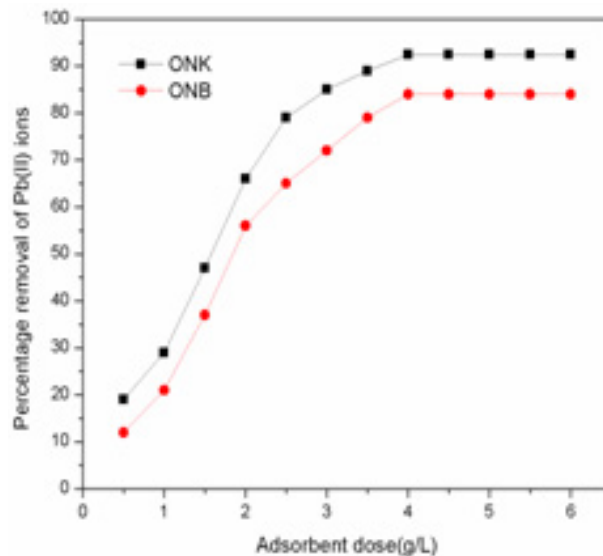


Fig. 12. Effect of adsorbent dosage on the adsorption of Pb(II) ions onto the ONK and ONB.

dosage [8]. Considering this fact, for the subsequent studies, 4 g/L was taken to be optimum. Comparing both the adsorbents, based on removal efficiency, ONK possesses less aggregation of adsorption sites leads to high surface area and the more number of the available sites for the adsorption of Pb(II) ions than ONB.

3.4. Effect of contact time

The contact time between the surface of the adsorbent material (solid phase) and a metal ion (liquid phase) is an important parameter in the adsorption process. The effect of contact time on the adsorption of Pb(II) ions on the adsorbents (ONK, ONB) was investigated and the results are shown in Fig. 13. It can be seen from Fig. 13, that the removal of Pb(II) ions highly increases at the initial stage of contact time and attains maximum removal efficiency of Pb(II) ions at 45 min for ONB (84%) and 30 min for ONK (92.4%). But due in the course of time, after which there is not any considerable significant variation in the removal of Pb(II) ions. Therefore, the contact time of 30 min (ONK) and 45 min (ONB) is optimized for further experimental studies. From the results, it is clear that the adsorption efficiency increases rapidly at the beginning due to the larger surface area of the adsorbents available for Pb(II) ions adsorption. As the capacity of the adsorbent gets exhausted, the adsorbed Pb(II) ions form a monolayer and then the uptake rate is controlled by the rate at which Pb(II) ions are transported from the exterior to the interior sites of the ONK, and ONB particles.

It is also evident that active sorption sites in the system have fixed number and each active sorption sites can absorb only one ion in a monolayer, the metal uptake by the sorbent is faster at the initial stage and gradually reduces down as the competition for the decreasing availability of active sites intensifies by the metal ion remaining in the solution [50].

3.5. Isotherm studies

The analysis of adsorption equilibrium data using Langmuir and Freundlich models for the removal of Pb(II) ions by ONB, ONK is shown in Table 2. Langmuir model is supported by the linear plot (Fig. 14) of C_e vs. C_e/Q_e that shows a better linear regression coefficient $R^2 = 0.99$ (ONK), 0.99 (ONB). This indicates the applicability of monolayer adsorption with maximum monolayer adsorption capacity (q_m) values of 47 mg/g (ONK) and 32.3 mg/g (ONB). The value of dimensionless separation factor R_L is between 0 and 1 indicate that adsorption of Pb(II) ions onto adsorbent is favorable. The separation factor values as obtained in Table 2, which are found in the range of 0–1 indicate that the adsorption is favorable in removing Pb(II) ions using both ONK and ONB adsorbents. Fig. 15 depicts the linear plot $\log Q_e$ vs. $\log C_e$ represents the linear regression coefficient $R^2 = 0.96$ (ONK), 0.95 (ONB) for the Freundlich model. The value of Freundlich constant K_f for ONK and ONB was found to be 2.47 and 2.15 respectively. In this case, the value of n is 3.07 for ONK and 3.04 for ONB which clearly indicates that the value of n is greater than 1, favorable for adsorption. In general, isotherm fitting yields good results with both Langmuir and Freundlich isotherm. However, Langmuir isotherm gives a better fitting than Freundlich isotherm, as there is a higher correlation coefficient as indicated in Langmuir isotherm.

The comparison of maximum monolayer adsorption capacity onto the various adsorbents is given in Table 3. The adsorption capacity of ONK is higher than other potential

adsorbents such as bael tree leaf, nano-silversol-coated activated carbon, raw cashewnut shell, chitosin-nanosize, chitosin-polyacrylonitrile blend for the adsorption of Pb(II) ions.

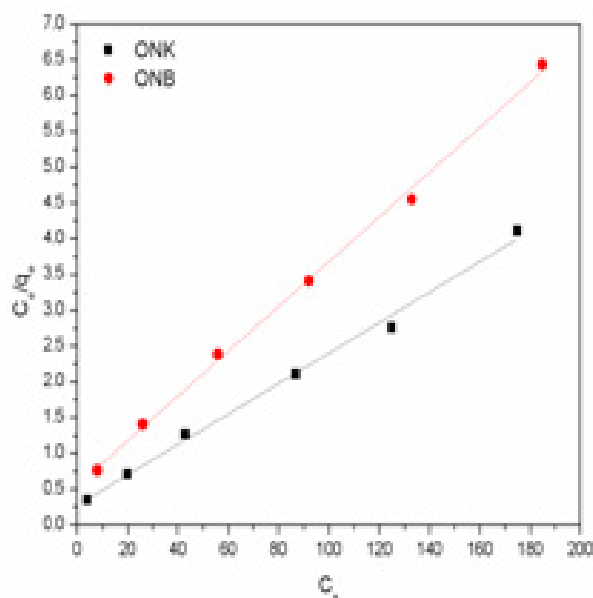


Fig. 14. Linear form of Langmuir isotherm (ONK, ONB).

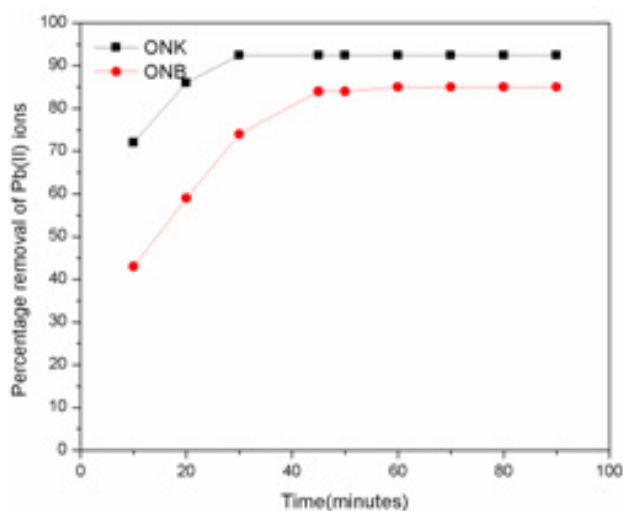


Fig. 13. Effect of contact time on the adsorption of Pb(II) ions onto the ONK and ONB.

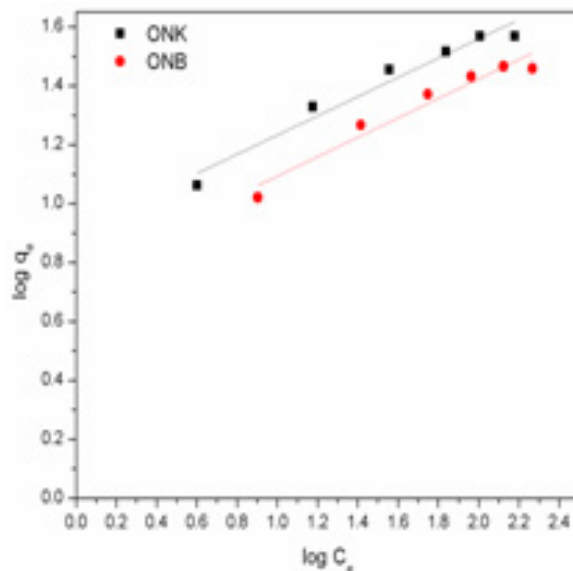


Fig. 15. Linear form of Freundlich isotherm (ONK, ONB).

Table 2
Parameters for Langmuir and Freundlich Isotherm

Parameters	Langmuir				Freundlich		
	$q_{m(cal)}$ (mg/g)	b (L/mg)	R_L	R^2	K_f ($mg^{1-1/n} L^{1/n} g^{-1}$)	n	R^2
ONK	47	0.07	0.03	0.99	2.47	3.07	0.96
ONB	32.3	0.06	0.04	0.99	2.15	3.04	0.95

3.6. Kinetic studies

In order to analyze the efficiency of adsorption, reaction rate and pathway pseudo-first order model and pseudo-second order model were tested to interpret the experimental data. The obtained parameters of pseudo-first and pseudo-second order model are summarized in Table 4. From Figs. 16,17, it is seen that the obtained correlation coefficient for the pseudo-first order model and pseudo-second order model are compared and the result shows that the pseudo-second order equation possesses higher correlation coefficient than pseudo-first order model. From the results revealed in Table 4, the calculated q_e value is compared with the experimental q_e value of the pseudo-first order model differs a lot, whereas in case of pseudo-second order model the calculated q_e is somewhat closer to the experimental q_e value. The result confirms that the adsorption kinetics of Pb(II) ions onto ONK, and ONB that is described by the pseudo-second order model

Table 3
Comparison of monolayer adsorption capacity of Pb(II) ions onto various adsorbents

Heavy metal	Adsorbent	q_m (mg/g)	References
Pb(II)	ONK	47	Present study
Pb(II)	ONB	32.3	Present study
Pb(II)	Bael tree leaf	4.06	16
Pb(II)	Nano-silversol-coated activated carbon	23.81	51
Pb(II)	Raw cashew nut shell	17.72	17
Pb(II)	Chitosin-nanosize	14.24	20
Pb(II)	Chitosin-Polyacrylonitrile blend	20.08	19
Pb(II)	<i>R. tortuosum</i>	60.15	12
Pb(II)	<i>Rhizocioniumhooleri</i>	81.7	54
Pb(II)	<i>Caryotaurens</i> seed	93.7	3
Pb(II)	Chitosin-functionalised magnetic nanoparticles	498.6	55
Pb(II)	Polyazomethinamide	452.1	52
Pb(II)	Cashew nut shell flakes	408.6	18
Cu(II)	Cashew nut shell flakes	406.6	56
Cd(II)	Cashew nut shell flakes	436.7	56
Zn(II)	Cashew nut shell flakes	455.7	56
Ni(II)	Cashew nut shell flakes	456.3	56
Pb(II)	<i>Guazumaulmifolia</i>	100	53
Pb(II)	<i>S. potatorum</i>	166.6	14

Table 4
Parameters for pseudo-first and pseudo-second order models

Parameters	Pseudo-first order				Pseudo-second order		
	$q_{e(exp)}$	$q_{e(cal)}$ (mg g ⁻¹)	$K_1 * 10^{-3}$ (min ⁻¹)	R ²	$q_{e(cal)}$ (mgg ⁻¹)	$K_2 * 10^{-3}$ (g mg ⁻¹ min ⁻¹)	R ²
ONK	38	3.3	8.75	0.87	30.33	3.41	0.98
ONB	30	6.2	1.08	0.87	21.73	4.20	0.96

is chemical adsorption and it is significant in the rate determining step.

3.7. Adsorption mechanism

To predict the rate-determining step and to understand the adsorption mechanism associated with adsorption phenomena, adsorption mechanism is necessary [57]. The adsorption process of Pb(II) ions onto the adsorbents ONK

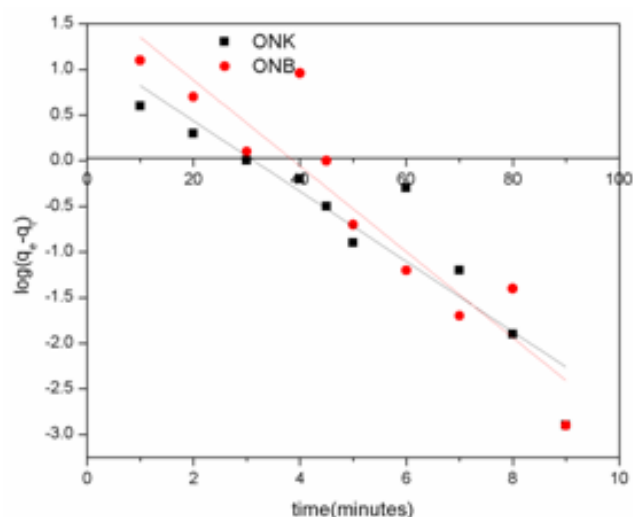


Fig. 16. Pseudo-first order-model (ONK, ONB).

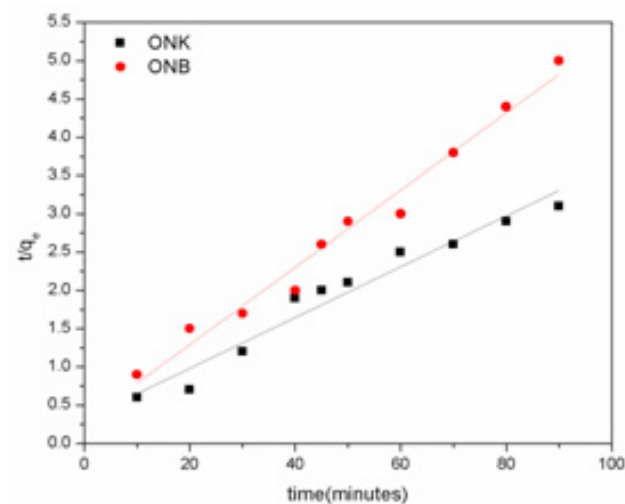


Fig. 17. Pseudo-second-order model (ONK, ONB).

and ONB dynamics can be explained by three consecutive steps.

- i. Transport of Pb(II) ions from bulk solution to the external surface of the ONK and ONB (film diffusion).
- ii. Pb(II) ions can move to the interior part of ONK and ONB particles (particle diffusion)
- iii. Adsorption of Pb(II) on the interior surface of the adsorbent pores and capillary surface.

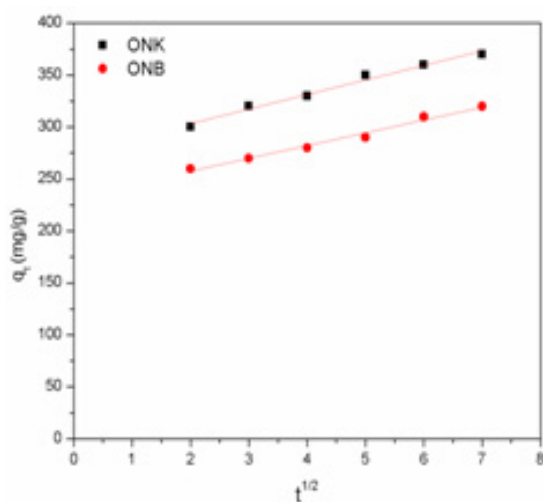


Fig. 18. Intra-particle diffusion model (ONK, ONB).

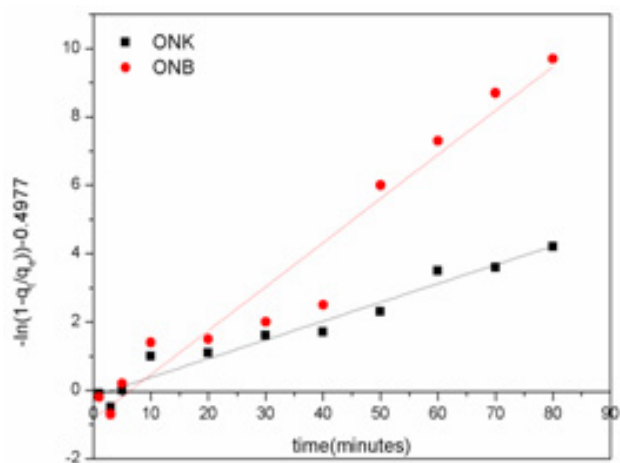


Fig. 19. Boyd model (ONK, ONB).

Table 5
Parameters for intra-particle diffusion and boyd kinetic model

Parameters	Intra-particle diffusion model			Boyd model		
	k_p (mg/g min ^{0.5})	C	R ²	B	$D_i \cdot 10^{-2}$ (m ² /s)	R ²
ONK	1.12	14.49	0.90	0.15	8.46	0.93
ONB	1.11	11.76	0.89	0.13	8.11	0.92

The overall rate of the reaction was examined using the slowest step involved in the adsorption process. It might be either film or particle diffusion. Initially, the adsorption of Pb(II) ions onto ONK and ONB may be controlled by film diffusion as the adsorbent gets loaded with Pb(II) ions. The process is controlled by intra-particle diffusion if intra-particle diffusion of Pb(II) ions are onto ONK, and ONB processes, then the system should have good mixing, large particle size of the adsorbent, high concentration of Pb(II) ions and low affinity of Pb(II) ions for ONK, ONB adsorbent. The kinetic results were tested by the intra-particle diffusion model to determine the particle diffusion mechanism and the results are shown in Figs. 18 and 19.

The first linear portion represents the boundary layer diffusion followed by another linear portion represents the intra-particle diffusion. The largest is the C value which is the contribution to the surface adsorption in the rate determining step. The plot q_t vs. $t^{1/2}$ is linear and passes through the origin, then intraparticle diffusion is the sole rate-determining step. But in this study, the linear plot does not pass through the origin. This indicates intra-particle diffusion is not the sole process takes place there is also some contribution of boundary layer diffusion. In order to identify this, the Boyd kinetic model is implemented. The linear plot of the Boyd kinetic model is shown in Fig. 19. Table 5 represents the corresponding parameter values of intra-particle diffusion and Boyd kinetic model.

4. Conclusion

In the present research work, the adsorption ability of ONK and ONB were tested for the removal of Pb(II) ions from the battery effluent. The batch adsorption process was affected by different operating parameters such as adsorbent dosage, pH, contact time. These adsorption parameters were optimized. Analysis of ONK, ONB by FTIR, TGA, XRD, SEM-EDX, revealed functional group, thermal stability, porous surface, abundant cationic elements that contributed to the adsorption of Pb(II) ions. Comparing both the adsorbents, ONK was found to be effective with 92.4% removal efficiency achieved at pH 4, at an adsorbent dosage of 4 g/L in 30 min contact time for 400 mg/L metal ion concentration. Adsorption isotherms Langmuir model and Freundlich model have been analyzed for obtained equilibrium data. Both the isotherms fit well with the process. The kinetic of adsorption of Pb(II) ions onto ONK, ONB was studied using pseudo-first order model, pseudo-second order model, intra-particle diffusion, and Boyd kinetic model. Kinetic

results showed that pseudo-second order model was the best adsorption kinetic model, which afford the best coefficient of determining value compared to other models and calculated $q_{e(cal)}$ was close to the experimental adsorption capacity, $q_{e(exp)}$. The external mass transfer control of Pb(II) removal was in the early stages and intra-particle at the latter stages. Boyd model confirmed that the external mass transfer was the slowest step involved in the adsorption process. Based on the results obtained from these studies, it can be concluded that ONK is an efficient and inexpensive adsorbent for the removal of Pb(II) ions than ONB.

Acknowledgment

The authors convey sincere thanks to the Management and Principal of Coimbatore Institute of Technology, Coimbatore-641014 for their support through the Technical Education Quality Improvement Programme (TEQIP-III) fund.

Symbols

B_i	— Mathematical function of F
C_i	— Constant related to the thickness of the boundary layer
C_0	— Initial Pb(II) ion concentration in the solution
C_e	— Final Pb(II) ion concentration in the solution
CTAB	— Cetyltrimethyl ammonium bromide
D_i	— Boyd model-effective diffusion coefficient of ion onto adsorbent (ONK, ONB) surface
EDX	— Energy dispersive X-ray
F	— Fraction of ion adsorbed onto the adsorbent (ONK, ONB) at any time t
FAA	— Flame atomic absorption spectrometer
FTIR	— Fourier transform infrared spectroscopy
HDTMA	— Hexadecyltrimethyl ammonium
k_1 (min^{-1})	— First order rate constant
k_2 ($\text{g mg}^{-1} \text{min}^{-1}$)	— Second order rate constant
K_f ($\text{mg}^{1-1/n} \text{L}^{1/n} / \text{g}$)	— Freundlich constants
ONK	— Organo-nanokaoline
ONB	— Organo-nanobentonite
q_e (mg/g)	— Amount adsorbed at equilibrium
q_m (mg/g), b (L/mg)	— Langmuir constants
q_i (mg g^{-1})	— Amount of adsorbate species adsorbed at equilibrium and at any time
r	— Boyd model-radius of the adsorbent
SEM	— Scanning electron microscope
TGA	— Thermogravimetric analyzer
TMA	— Tetra-methyl ammonium

TEA	— Tetra-ethyl ammonium
TBMA	— Tribenzylmethyl-ammonium
XRD	— X-ray diffraction

References

- [1] U. Pearlin Kiruba, P. Senthil Kumar, K. Sangita Gayatri, S. Shahul Hameed, M. Sindhuja, C. Prabhakaran, Study of adsorption kinetic, mechanical, isotherm, thermodynamic and design models for Cu (II) ions on sulfuric acid-modified Eucalyptus seeds: temperature effect, Desal. Water Treat., 56 (2015) 2948–2965.
- [2] U. Pearlin Kiruba, P. Senthil Kumar, C. Prabhakaran, V. Aditya, Characteristics of thermodynamic, isotherm, kinetic, mechanism and design equations for the analysis of adsorption in Cd(II) ions-surface modified *Eucalyptus* seeds system, J. Taiwan Inst. Chem. Eng., 45 (2014) 2957–2968.
- [3] S. Anbalagan, P. Senthil Kumar, S.R.P. Selvam, A. Sankaranarayan, A. Dutta, Influence of ultrasonication on preparation of novel material for heavy metal removal from wastewater, Korean J. Chem. Eng., 33 (2016) 2716–731.
- [4] K. Anbalagan, P. Senthil Kumar, K. Sangita Gayatri, S. Shahul Hameed, M. Sindhuja, C. Prabhakaran, R. Karthikeyan, Removal and recovery of Ni(II) ions from synthetic wastewater using surface modified *Strychnospotatorum* seeds: experimental optimization and mechanism, Desal. Water Treat., 53 (2015) 171–182.
- [5] K. Anbalagan, P. SenthilKumar, R. Karthikeyan, Adsorption of toxic Cr(VI) ions from aqueous solution by sulphuric acid modified *Strychnospotatorum* seeds in batch and column studies, Desal. Water Treat., 57 (2015) 12585–12607.
- [6] P. Senthil Kumar, Adsorption of Zn(II) ions from aqueous environment by surface modified *Strychnospotatorum* seeds, a low cost adsorbent, Polish J. Chem. Technol., 15 (2013) 35–41.
- [7] P. Senthil Kumar, A. Saravanan, K. Anish Kumar, R. Yashwanth, S. Visvesh, Removal of toxic zinc from water/wastewater using *eucalyptus seeds* activated carbon: non-linear regression analysis, IET Nanobiotechnol., 10 (2016) 244–253.
- [8] P. Senthil Kumar, A.S.L. Sai Deepthi, R. Bharani, C. Prabhakaran, Adsorption of Cu(II), Cd(II) and Ni(II) ions from aqueous solution by unmodified *Strychnospotatorum seeds*, Europ. J. Environ. Civil Eng., 17 (2013) 293–314.
- [9] G. Neeraj, S. Krishnan, P. Senthil Kumar, K.R. Shriaiashvarya, V. Vinoth Kumar, Performance study on sequestration of copper ions from contaminated water using newly synthesized high effective chitosan coated magnetic nanoparticles, J. Molec. Liq., 214 (2016) 335–346.
- [10] V.N. Thekkudan, V.K. Vaidyanathan, P. Senthil Kumar, C. Christy, S. SaiLavanyaa, D. Vishnu, S. Anbalagan, V.K. Vaithyanathan, S. Subramanian, Review on nanoadsorbents: a solution for heavy metal removal from wastewater, IET Nanobiotechnol., 11 (2016) 213–224.
- [11] US Environmental Protection Agency (UEPA), Environmental Pollution Control Alternatives: Drinking Water Treatment for Small Communities, USEPA, Washington, Dc, 1990.
- [12] S. Suganya, K. Kayalvizhi, P. Senthil Kumar, A. Saravanan, V. Vinoth Kumar, Biosorption of Ni(II) and Cr(VI) ions from aqueous solution using *Rhizocloniumtortuosum*: extended application to nickel plating industrial wastewater, Desal. Water Treat., 57 (2016) 25114–25139.
- [13] P.K. Pandey, S.K. Sharma, S.S. Sambhi, Removal of lead(II) from waste water on zeolite-NaX, J. Environ. Chem. Eng., 3(2015) 2604–2610.
- [14] P. Senthil Kumar, C. Senthamarai, A.S.L. Sai Deepthi, R. Bharani, Adsorption isotherms, kinetics and mechanism of ions removal from aqueous solution using chemically modified agricultural waste., Canad. J. Chem. Eng., 91(2013) 1950–1956.

- [15] L. Largitte, J. Laminie, Modelling the lead concentration decay in the adsorption of lead onto a granular activated carbon, *J. Environ. Chem. Eng.*, 3 (2015) 474–481.
- [16] P. Senthil Kumar, R. Gayathri, Adsorption of Pb^{2+} ions from aqueous solutions onto Bael tree leaf powder: Isotherms, kinetics and thermodynamics study, *J. Eng. Sci. Technol.*, 4 (2009) 381–399.
- [17] P. Senthil Kumar, Adsorption of lead(II) ions from simulated wastewater using natural waste: A kinetic, thermodynamic and equilibrium study, *Environ. Progr. Sustain. Energy*, 33 (2013) 55–64.
- [18] P. Senthil Kumar, S. Ramalingam, R.V. Abhinaya, K.V. Thiruvengadaravi, P. Baskaralingam, S. Sivanesan, Lead(II) adsorption onto sulphuric acid treated cashew nut shell, *Separ. Sci. Technol.*, 46 (2011) 2436–2449.
- [19] T. Anitha, P. Senthil Kumar, K. Sathish Kumar, B. Ramkumar, S. Ramalingam, Adsorptive removal of ions from polluted water by newly synthesized chitosan–polyacrylonitrile blend: Equilibrium, kinetic, mechanism and thermodynamic approach, *Process Safety Environ. Protect.*, 98 (2015) 187–197.
- [20] T. Anitha, P. Senthil Kumar, K. Sathish Kumar, K. Sriram, J. Feroze Ahmed, Biosorption of lead(II) ions onto nano-sized chitosan particle blended polyvinyl alcohol (PVA): adsorption isotherms, kinetics and equilibrium studies, *Desal. Water Treat.*, 57 (2015) 13711–13721.
- [21] V. Kanchana, T. Gomathi, V. Geetha, Adsorption analysis of by nanocomposites of chitosan with methyl cellulose and clay, *J. Pharm. Biol. Res.*, 4 (2012) 1071–1079.
- [22] G. Tan, H. Yuan, Y. Liu, D. Xiao, Removal of lead from aqueous solution with native and chemically modified corncobs, *J. Hazard. Mater.*, 174 (2010) 740–745.
- [23] T. Suopajarvi, H. Liimatainen, M. Karjalainen, H. Upola, J. Niinimaki, Lead adsorption with sulfonated wheat pulp nano celluloses, *J. Water Process Eng.*, 5 (2015) 136–142.
- [24] G.M. Joziane, P.M. Muril, K. Thirugnanasambandham, H.B.F. Sergio, L.G. Marcelino, A.S.D.B. Maria, V. Sivakumar, Preparation and characterization of calcium treated bentonite clay and its application for the removal of lead and cadmium ions: Adsorption and thermodynamic modeling, *Process Safety Environ. Protect.*, 111 (2017) 244–252.
- [25] V. Masindi, W.M. Gitari, Simultaneous removal of metal species from acidic aqueous solutions using cryptocrystalline magnesite/bentonite clay composite: An experimental and modeling approach, *J. Cleaner Prod.*, 112 (2016) 1077–1085.
- [26] L.S. Gaona Galindo, A.F. de Almeida Neto, M.G.C. da Silva, M.G. AdeodatoVieira, Removal of cadmium(II) and lead(II) ions from aqueous phase on sodic bentonite, *Mater. Res.*, 16 (2013) 515–527.
- [27] M.R. Khan, R.A. Hegde, M.A. Shabiiimam, Adsorption of lead by bentonite clay, *Int. J. Scient. Res. Manage.*, 5 (2017) 5800–5804.
- [28] K. Bellir, M.B. Lehocine, A.-H. Meniai, Zinc removal from aqueous solutions by adsorption onto bentonite, *Desal. Water Treat.*, 51 (2013) 5035–5048.
- [29] B. Meroufel, O. Benali, M. Benyahia, M.A. Zenasni, A. Merlin, B. George, Removal of Zn(II) from aqueous solution onto kaolin by batch design, *J. Water Resour. Protect.*, 5 (2013) 669–680.
- [30] M.-q. Jiang, X.-y. Jin, X.-q. Lu, Z.-l. Chen, Adsorption of Cd(II), Ni(II) and Cu(II) onto natural kaolinite clay, *Desalination*, 252 (2010) 33–39.
- [31] S.A. Drweesh, N.A. Fathy, M.A. Wahba, A.A. Hanna, A.I.M. Akarish, E.A.M. Elzahany, I.Y. El-Sherif, K.S. Abou-El-Sherbini, Equilibrium, kinetic and thermodynamic studies of adsorption from aqueous solutions on HCl-treated Egyptian kaolin, *J. Environ. Chem. Eng.*, 4 (2016) 1674–1684.
- [32] K. Al-Essa, F. Khalili, Heavy metals adsorption from aqueous solutions onto unmodified and modified Jordanian kaolinite clay: batch and column techniques, *Amer. J. Appl. Chem.*, 6 (2018) 25–34.
- [33] K.R. Kumric, A.B. Dukic, T.M. Trtic-Petrovic, N.S. Vukelic, Z. Stojanovic, J.D. GrbovicNovakovic, L.L. Matovic, Simultaneous removal of divalent heavy metals from aqueous solutions using raw and mechanochemically treated interstratified montmorillonite/kaolinite clay, *Ind. Eng. Chem. Res.*, 52 (2013) 7930–7939.
- [34] M.-q. Jiang, Q.-p. Wang, X.-y. Jin, Z.-l. Chen, Removal of from aqueous solution using modified and unmodified kaolinite clay, *J. Hazard. Mater.*, 170 (2009) 332–339.
- [35] E. Ruiz-Hitzky, P. Aranda, M. Dardera, G. Rytwo, Hybrid materials based on clays for environmental and biomedical applications, *J. Mater. Chem.*, 20 (2010) 9306–9321.
- [36] S.S. Bhattacharya, M. Aadhar, Studies on preparation and analysis of organoclay nano particles, *Res. J. Eng. Sci.*, 3 (2014) 10–16.
- [37] W. Chen, H.-c. Liu, Adsorption of sulfate in aqueous solutions by organo-nano-clay: Adsorption equilibrium and kinetic studies, *J. Central South Univ.*, 21 (2014) 1974–1981.
- [38] A. Hassania, A. Khataeb, S. Karaca, M. Shirzad-Siboni, Surfactant-modified montmorillonite as a nanosized adsorbent for removal of an insecticide: Kinetic and isotherm studies, *Environ. Technol.*, 36 (2015) 3125–3135.
- [39] M. Shirzad-Siboni, A. Khataee, A. Hassani, S. Karaca, Preparation, characterization and application of a CTAB-modified nanoclay for the adsorption of an herbicide from aqueous solutions: Kinetic and equilibrium studies, *Comptes Rendus Chimie*, 18 (2015) 204–214.
- [40] M. Kirans, R. Darvishi, C. Soltani, A. Hassani, S. Karaca, A. Khataee, Preparation of cetyltrimethyl ammonium bromide modified montmorillonite nanomaterial for adsorption of a textile dye, *J. Taiwan Inst. Chem. Eng.*, 45 (2014) 2565–2577.
- [41] Langmuir, The adsorption of gases on plane surfaces of glass, mica, and platinum, *J. Amer. Chem. Soc.*, 40 (1918) 1361–1368.
- [42] H.M.F. Freundlich, Over the adsorption in solution, *J. Phys. Chem.*, 57 (1906) 385–471.
- [43] S. Lagergren, About the theory of so-called adsorption of soluble substances, *Kungliga Svenska VetenskHandl.*, 24 (1898) 1–39.
- [44] Y.S. Ho, G. McKay, Pseudo-second order model for sorption processes, *Process Biochem.*, 34 (1999) 451–465.
- [45] W.J. Weber, J.C. Morris, Kinetics of adsorption on carbon from solution, *J. Sanit. Eng. Div. Amer. Soc. Civil Eng.*, 89 (1963) 31–60.
- [46] G.E. Boyd, A.W. Adamson, L.S. Myers, The exchange adsorption of ions from aqueous solutions by organic zeolites. II. Kinetics, *J. Amer. Chem. Soc.*, 69 (1947) 2836–2848.
- [47] S. Suganya, P. Senthil Kumar, Influence of ultrasonic waves on preparation of active carbon from coffee waste for the reclamation of effluents containing Cr(VI) ions, *J. Ind. Eng. Chem.*, 60 (2018) 307–320.
- [48] S. Karaca, A. Gurses, M.E. Korucu, Investigation of the orientation of CTA⁺ ions in the interlayer of CTAB pillared montmorillonite, *J. Chem.*, 2013 (2012) 1–10.
- [49] P. SenthilKumar, C. Senthamarai, A. Durgadevi, Adsorption kinetics, mechanism, isotherm, and thermodynamic analysis of copper ions onto the surface modified agricultural waste, *Environ. Progr. Sustain. Energy.*, 33 (2012) 28–37.
- [50] P. SenthilKumar, S. Ramalingam, R.V. Abhinaya, S. Dinesh Kirupha, T. Vidhyadevi, S. Sivanesan, Adsorption equilibrium, thermodynamics, kinetics, mechanism, and process design of zinc(II) ions onto cashew nut shell, *Canad. J. Chem. Eng.*, 90 (2011) 973–982.
- [51] P. Senthil Kumar, C. Vincent, K. Kirthika, K. Sathish Kumar, Kinetics and equilibrium studies of Pb^{2+} ion removal from aqueous solutions by use of nano-silversol-coated activated carbon, *Brazil. J. Chem. Eng.*, 27 (2010) 339–346.
- [52] A. Murugesan, L. Ravikumar, V. Sathya Selva Bala, P. Senthil Kumar, T. Vidhyadevi, S. Dinesh Kirupha, S.S. Kalaivani, S. Krithiga, S. Sivanesan, Removal of Pb(II), Cu(II) and Cd(II) ions from aqueous solution using poly azomethine amides: Equilibrium and kinetic approach, *Desalination*, 271 (2011) 199–208.
- [53] P. Rajkumar, P. Senthil Kumar, S. Dinesh Kirupha, T. Vidhyadevi, J. Nandagopal, S. Sivanesan, Adsorption of ions onto surface modified *Guazumaumifolia* seeds and batch adsorber design, *Environ. Progr. Sustain. Energy.*, 32 (2012) 307–316.

- [54] S. Suganya, A. Saravanan, P. Senthil Kumar, M. Yashwanthraj, P. Sundar Raja, K. Kayalvizhi, Sequestration of and Ni(II) ions from aqueous solution using microalga *Rhizocloniumhookeri*: adsorption thermodynamics, kinetics, and equilibrium studies, *J. Water Reuse Desal.*, 7 (2016) 214–227.
- [55] F.C. Christopher, S. Anbalagan, P. Senthil Kumar, S. Rajan Pannerselvam, V.K. Vaidyanathan, Surface adsorption of poisonous ions from water using chitosan functionalized magnetic nanoparticles, *IET Nanobiotechnol.*, 11 (2017) 433–442.
- [56] P. Senthil Kumar, S. Ramalingam, R.V. Abhinaya, S.D. Kirupha, A. Murugesan, S. Sivanesan, Adsorption of metal ions onto the chemically modified agricultural waste, *Clean – Soil, Air, Water.*, 40 (2012) 188–197.
- [57] P. Senthil Kumar, S. Ramalingam, S. Dinesh Kirupha, A. Murugesan, T. Vidhyadevi, S. Sivanesan, Adsorption behavior of nickel(II) onto cashew nut shell: Equilibrium, thermodynamics, kinetics, mechanism and process design, *Chem. Eng. J.*, 167 (2011) 122–131.